Metabolic Alterations in Meningioma Reflect Clinical Course

Waseem Masalha (waseem.masalha@uniklinik-freiburg.de)
Freiburg University Hospital: Universitatsklinikum Freiburg https://orcid.org/0000-0001-5581-8764
Karam Daka
Freiburg University Hospital: Universitatsklinikum Freiburg
Jakob Woerner
Universitätsklinikum Freiburg: Universitatsklinikum Freiburg
Nils Pompe
Universitatsklinikum Freiburg
Stefan Weber
Universitatsklinikum Freiburg
Daniel Delev
Universitätsklinikum Aachen: Universitatsklinikum Aachen
Marie T. Krueger
Kantonsspital Sankt Gallen
Oliver Schnell
Freiburg University Hospital: Universitatsklinikum Freiburg
Jürgen Beck
Freiburg University Hospital: Universitatsklinikum Freiburg
Dieter Henrik Heiland
Freiburg University Hospital: Universitatsklinikum Freiburg
Juergen Grauvogel
Freiburg University Hospital: Universitatsklinikum Freiburg

Research article

Keywords: Tumor metabolism, Meningioma

Posted Date: October 9th, 2020

DOI: https://doi.org/10.21203/rs.3.rs-87461/v1

Version of Record: A version of this preprint was published on March 1st, 2021. See the published version at https://doi.org/10.1186/s12885-021-07887-5.

Abstract

Background

Meningiomas are common brain tumors, defined by an innocent clinical course. However, some meningiomas reveal a malignant transformation and recur within a short time period regardless of their WHO grade. The current study aims to identify potential markers, which can discriminate between benign and malignant meningioma courses.

Methods

For this purpose, we profiled the metabolites of 43 patients with low- and high-grade meningiomas. Tumor specimens were analyzed by NMR analysis; 270 metabolites were identified and clustered with the AutoPipe algorithm.

Results

We observed two distinct clusters marked by alterations in the glycine-serine, choline or tryptophan metabolism. Both clusters showed significant differences between WHO graduation and proliferation index.

Conclusion

Our findings suggest that alterations of glycine-serine are associated with a lower proliferation and frequencies of recurrent tumors. Alterations of the choline-tryptophan metabolism causes increased proliferation and recurrence is more common. Our results suggest, that tumor malignancy is reflected by metabolic alterations, which can support histological classifications in order to predict the clinical outcome of patients with meningiomas.

Background

Meningiomas are common brain tumors in adults that account for 13–26% of all intracranial tumors (1). The 2016 World Health Organization (WHO) classification divided meningiomas into three histological grades (I to III) and described 16 histopathological subtypes (2). These WHO grades present a significant correlation with clinical outcome in several recent studies. The majority of meningiomas are benign tumors (90%) mainly treated by surgery, followed by an innocent clinical course (1). Atypical meningioma (WHO grade II) reveal worse clinical outcome due to higher recurrence rates of up to 30–40% (2). Additionally, a small subset of meningiomas (1–2.8%) is classified as anaplastic meningiomas showing a particularly aggressive clinical course and a recurrence rate of nearly 100% (1).

However, a few of all benign meningiomas (WHO grade I) transform into an aggressive growth pattern and recur after a short period of time (3). In order to address the variety of clinical outcomes within the WHO grade I group, multiple groups investigated the genetic landscape of meningiomas and showed

region-specific genomic alterations (4). Therefrom, five genetic subgroups were identified based on transcriptional similarity and associated mutational patterns. Most frequently, meningiomas contained an *NF2, SMARCB1 (Group1), TRAF7/KLF4 (Group2)* and *PI3K (Group3)* mutation, which drive WNT-pathway activation. In another group, Hedgehog pathway activation was detected by transcriptional profiles and mainly based on mutations such as *SMO* (5). The last subgroup was identified by meningiomas, which showed a distinct mutation in the *POLR2A* gene followed by a dysregulation of RNA synthesis (4). (6–9). Beside genomic alteration, tumor metabolism was recently described as a hallmark driver of malignancy and tumor development. Different tumor entities, including brain and other solid tumors, showed numerous metabolic alterations. In meningiomas, Monleon and colleagues described a strong association between altered tumor metabolism and chromosomal instability. These metabolic alterations were found to be irrespective of the WHO grade (10). Other authors confirmed these findings and linked metabolic aggressiveness to distinct genetic and molecular alterations. Serna *et al.*, showed that metabolic aggressiveness was driven by alterations in the expression of *IGF1R* (Insulin-Growth-Factor1-Receptor), which is involved in the regulation of glycolysis (11). Following the hypothesis of altered glycolysis in meningiomas, it was shown that different parts of the glycolysis are transformed, including PFK (phosphofructokinase) and LDH (lactate dehydrogenase), which were significantly increased in anaplastic meningioma compared to other histological subtypes (12). Additionally, alterations of the tryptophan metabolism were uncovered, which force the immune-escape mechanism to an increased activity of the kynurenine-pathway (13), (14). Today, increased opportunities in bioinformatics and metabolic profiling allow detecting associations between metabolic networks and clinical parameters to predict metabolic patterns and associated clinical outcome parameters. Our aim was to identify benign and potential malignant transformed meningiomas within the defined WHO grade I by metabolic profiling and computational analysis.

Methods

Contact for reagent and resource sharing

Further information and requests for resources, raw data and reagents should be directed and will be fulfilled by contacting D. H. Heiland, dieter.henrik.heiland@uniklinik-freiburg.de. A full table of all materials is given in the supplementary information.

Ethical Approval

For this study, we included 43 patients who underwent surgery at the Department of Neurosurgery of the Medical Center, University of Freiburg. The local ethics committee of the University of Freiburg approved data evaluation, imaging procedures and experimental design (protocol 100020/09 and 5565/15). The methods were carried out in accordance with the approved guidelines. Written informed consent was obtained. The studies were approved by an institutional review board.

Imaging, Tissue Collection and Histology

Tumor tissue was sampled from the meningioma core, snap-frozen in liquid nitrogen immediately after resection and processed for further metabolic analysis. Representative tissue samples of all samples were fixed using 4% phosphate buffered formaldehyde and paraffin-embedded through standard procedures. Haemotoxylin and Eosin (H&E) staining was performed on 4 µm paraffin sections using standard protocols. These stainings confirmed the correct sampling.

Metabolite Extraction and ^{1}H-NMR Analysis

Metabolites were extracted with 400 µl ice-cold 80% methanol and 400 µl ice-cold water, homogenized by a tissue grinder (VWR, Radnor, USA) and sonicated in 1 °C, then centrifuged at 15,000 × *g* for 20 minutes to remove proteins. Extracts were dried by lyophilization and resuspended in 650 µl deuterated water as described in Beckonert *et al*. (15). 600 µl suspension was transferred to NMR tubes for further NMR procedures. ^{1}H-NMR spectra were collected at the Institute of Physical Chemistry of the University of Freiburg with a Bruker Avance III HDX 600-MHz NMR spectrometer (Bruker, Rheinstetten, Germany), equipped with a PABBO BB/19F-1H/D Z-GRD probe head. Each individual spectrum was recorded with two dummy scans and 32 scans with 64 k points in the time domain. The sweep width was set to 16.02 ppm with an offset of 4.691 ppm. This resulted in an acquisition time of 3.4 seconds for each scan with a dwell time of 52 microseconds. The relaxation delay was set to 2 seconds for acquisition, and the water signal was suppressed by an excitation sculpting scheme (16).

Postprocessing of Metabolic Data

In order to adjust the spectra from multiple batches, spectra were manually aligned by setting the peak of L-lactate acid at 1.310 ppm. All acquisition and processing of the spectra were performed with TopSpin 3.2 patch level 6. Detailed description of the methods was given in a recent published study by Heiland *et al*. (17). All spectra were analyzed with the software package “batman”, an R-software-based tool for metabolite detection in complex spectra (18). The batman software fits a predefined list of metabolites by a Bayesian approach. A detailed description of the batman algorithm was given by Hao *et al*. (18). Normalization of the spectra was performed by pseudo-counted Quantile (pQ) Normalization algorithm integrated in the KODAMA package. Further processing of metabolic data is described in the specific method section below.

Cluster Analysis

Normalized metabolic data was processed with AutoPipe (https://github.com-/heilandd/AutoPipe), a software package for automated unsupervised clustering. First, the number of subgroups was computed by “Partitioning Around Medoids” (Cluster number $k = 2–12$). To identify the optimal number of clusters, we calculated the mean silhouette width of each cluster composition. Next, to identify the core samples of each cluster, samples with a negative silhouette width were removed from further analysis. We then used either the PAMR(19) algorithm, a machine-learning based method, or a generalized linear model (20) to identify characteristic up- or downregulated metabolites of each subgroup.

Weighted Correlation Network Analysis (WCNA)

WCN-Analysis is a robust tool for integrative network analysis and was used in recent studies (21–23). It is based on a scaled-topology-free based network approach and uses the topological overlapping measurement to identify corresponding modules. These modules were analyzed by their eigengene correlation to each metabolite. The correlation of the intramodule connectivity (kME) and metabolites was used as input for a “Cluster of Clusters Analysis”. This analysis integrates expression modules and metabolites, which present equal correlation values (kME and metabolite intensity values). A detailed description of WCNA is given in (24).

Functional Analysis

Metabolic data was processed by pathviewer, an R package that includes KEGG pathway maps (25). Expression data (as described above) and normalized, log2 transformed and median centered metabolic data were integrated in the pathviewer algorithm. Enrichment analysis of metabolic data was performed with DOSE package and the web-based tool MetaboAnalyst 3.0 (www.metaboanalyst.ca).

Results

Meningiomas reveal two distinct metabolic clusters

We started our investigation by purifying metabolites from 43 meningiomas localized at different anatomic regions, including the convexity in 12 cases (27.9%), the falcine site in 6 cases (13.9%), the sphenoid ridge in 6 cases (13.9%), the frontobasal region in 9 cases (20.9%), the petroclival region in 2 cases (4.6%), the spinal site in 3 cases (6.9%), and 5 cases at other regions. The histopathological analysis showed 28 patients with meningiomas WHO grade I (65.1%), 12 with meningiomas WHO grade II (27.9%) and 3 patients with meningiomas WHO grade III (6.9%). Two patients with meningioma WHO grade II and three patients with meningioma WHO grade III showed a tumor recurrence within one year. 24 (55.9%) patients had a proliferation index (MIB-1) below 5% and 19 (44.1%) patients had a proliferation index (MIB-1) above 5%. A gross total resection (Simpson grade 1 + 2) was achieved in 37 patients and a subtotal resection (Simpson grade 3 + 4) was achieved in 6 patients. A detailed overview of all parameters can be found in Table 1.

Metabolites were analyzed using NMR and processed by a comprehensive computational analysis (Fig. 1). We, first, conducted an unsupervised cluster analysis of the top 100 most variable metabolites by PAM clustering. The optimal number of clusters was defined by maximal mean silhouette widths (Fig. 2 A-B). Therefrom, the analysis revealed two distinct clusters. In the first cluster, named “Metabolic Cluster I”, we found an up-regulated glycine/serine metabolism with the major signature metabolites glycine, serine and arginine. Patients of this cluster were exclusively histologically grade I and showed a significant lower rate of edema ($p < 0.05$) and this cluster showed a low proliferation rate (mean 1.2, IQR 0.3, $p < 0.05$). The second cluster (Metabolic Cluster II) was found to be easily separated into two subclusters by PAM clustering. On one side it contained patients with a medium proliferation rate of 2.1

IQR 0.7 and increased edema compared to cluster 1 ($p < 0.05$) (Fig. 2 A-B). The cluster specific pathway was found to be choline metabolism. On the other side, we found an increased tryptophan metabolism and also a strong activation of the choline pathway in the second subcluster. In this cluster, the proliferation rate was massively increased (mean 11.7, IQR 4.3, $p < 0.05$) and edema was observed in most of the patients. We found a high incidence of meningioma WHO grade II ($n = 12$) and III ($n = 3$) but also meningioma WHO grade I ($n = 13$) (Fig. 2 A-B).

Weighted Correlation Network Analysis of Metabolic Profiles in Meningiomas

We aimed to characterize the metabolic pathways in detail and performed a weighted correlation network analysis of metabolic profiles. Five metabolic modules were identified (Fig. 2C). Three modules showed a strong association with the WHO grade based on a logistic model, included WHO graduation and module eigengene. Therefrom, module GI (associated with WHO Grade I, $R = 0.25$, $p_{adj}=0.05$), module GII (associated with WHO Grade II, $R = 0.26$, $p_{adj}=0.05$) and module GIII (associated with WHO Grade III, $R = 0.28$, $p_{adj}=0.01$) were taken into consideration for further analysis. The other modules failed to achieve a significant correlation with the WHO grading. First, we analyzed the correlation between GI module eigengene and clinical features (Figure S1A). We found a significant negative correlation between module GI and perifocal edema (R -0.3, $p_{adj}=0.01$) and the histological defined atypical meningiomas (R -0.38, $p_{adj}=0.03$), which confirmed our findings. Meningiomas with a module GI signature were mostly observed in the convexity (R -0.32, $p_{adj}=0.04$). The histological subtype of a “transitional meningioma“ was highly significant associated with the GI signature (R -0.41, $p_{adj}=0.001$). Next, we examined the enrichment of metabolic pathways in each module. A metabolite set enrichment analysis (MSEA) showed a significant up-regulation of the glycine-serine pathway (*Enrichment Score*: 1.75, *p-value*: 0.0067) and glutamate metabolism (*Enrichment Score*: 1.52, *p-value*: 0.047), (Figure S1B). We computed a network based on the metabolites of the module GI. Connections within the network were based on intramodule connectivity. Therefrom, we identified the amino acids serine, glycine and the metabolite creatine as metabolic key-players in grade I meningiomas. In a next step, we examined the correlation between GII module eigengene and clinical features (Figure S2A). We found a significant correlation between module GII and perifocal edema (R 0.25, $p_{adj}=0.05$) and the histological defined atypical meningioma (R 0.41, $p_{adj}=0.02$). No correlation between localization and module eigengene was observed. The metabolic network of module GII identified tryptophan and kynurenic acid as hub-metabolites (Figure S2B). In line with the network findings, a metabolic pathway analysis uncovered an up-regulation of the tryptophan metabolism pathway (*Enrichment Score*: 1.83, *p-value*: 0.0093), (Fig. 2C). In order to characterize module GIII, we examined the correlation between module eigengene and clinical features (Figure S2D). No clinical feature was associated with this module, except the WHO grading (R 0.28, $p_{adj}=0.01$). Additionally, no correlation between localization and module eigengene was found. We next computed a network of metabolites of module GIII. Choline, iso-leucine and sphingosine identified as hub-metabolites, (Figure S2E). In line with the network findings, a metabolic pathway analysis uncovered an up-regulation of the choline metabolism pathway (*Enrichment Score*: 1.06, *p-value*: 0.0014).

Discussion

Due to favorable clinical course, most meningiomas are classified as benign. Although they are characterized as benign, 20% of patients within this subgroup reveal a tumor recurrence, even after gross total resection (3). These subtypes of tumors are difficult to identify and challenging for future treatment. To better predict their clinical outcome previous studies performed metabolic analysis by high resolution magic angle spinning (HR-MAS) and reported a correlation between metabolic and WHO graduation of meningiomas (10, 26), however they were limited by a small number of observed metabolites. We aimed to investigate a global metabolic profiling in order to identify specific subgroups, which were driven by unique metabolic alterations and associated with WHO grades. In the presented study, we performed an ex-vivo metabolic profiling by NMR spectroscopy of meningioma specimens, including all WHO grades (I, II and III), followed by computational detection of metabolites and cluster analysis. Our cluster analysis identified two major metabolic cluster, of which one cluster was divided into two subclusters of meningiomas based on the top 100 most varying metabolites. The first metabolic cluster was highlighted by serine and glycine metabolism, which provide a basis for synthesis of other amino acids, proteins as well as lipids. Their metabolism could increase the anti-oxidative capacity and reduce cellular reactive oxygen species (ROS). In particular, the glycine cleavage system fuels the mono-carbon metabolism yielding within a complex cellular network based on folate compound reactions, which play a central role in cellular redox balance over modulation of the $NADP^+$/NADPH-ratio (27). This network is also an essential component of methylation reactions that may be relevant for the maintenance of the cellular epigenetic status (28). In our study serine and glycine metabolisms were associated with benign meningiomas (WHO grade I) and a significantly low proliferation index ($p = 0.01$). This cluster was also accompanied by significantly lower edema in the magnetic resonance imaging ($p = 0.02$), **(Fig. 2, Table 1)** when compared to higher grades. The role of glycine in meningiomas is controversially discussed. While some authors reported a complete absence of glycine in aggressive meningioma (29), others showed a significantly increased glycine/alanine ratio. Furthermore a significantly increased ratio of glycine to glutamine/glutamate in rapidly recurrent meningiomas and an increased glycine value in benign meningioma has been observed (30, 31). In contrast, Monleon and colleagues found increased glycine levels in atypical meningiomas due to hypothesized increased angiogenesis (10). These discrepancies of glycine levels within different studies suggest the existence of more complex subgroups within the pathological delineation of grade I meningiomas. In line with published data, we have detected glycine-serine metabolism in a subgroup of benign meningioma. Other clusters also contain grade I tumors, which results in an inaccuracy of individual metabolic levels within the pathologic delineation grade I meningioma. The second metabolic cluster was defined by choline and tryptophan metabolism. Choline is an important component of the cell membrane. Higher choline concentrations are usually present in brain tumors compared to normal brain tissue. Thereby, choline acts as a brain tumor marker (32). Elevated choline peaks can also be detected in regions with high tumor cell density, in which the tissue is not necessarily anaplastic (33). The increased rate of proliferation, which was observed in tumors of the second cluster, consequently drives the choline metabolism due to increased demand of membrane components. Previous findings suggested that choline levels are significantly increased in benign

meningioma with aggressive clinical course (10, 11). Further, Mishra and colleagues reported high choline levels in malignant meningioma (34). In contrast, others reported a prominent choline level in meningioma WHO grade I. They did not observe differences of choline concentrations within all WHO grades, however, only a small number of WHO grade II + III meningioma were included in their study (30). We, further, identified the tryptophan metabolism, which is metabolized mainly by three pathways such as the serotonin (5-Hydroxytryptamine; 5-HT) pathway, the kynurenine (KYN) pathway and the tryptamine pathway (35). It has been reported that an overexpression of tryptophan catabolizing enzymes indoleamine 2,3-dioxygenase 1/2 or tryptophan 2,3-dioxygenase are associated with tumor progression. These two enzymes convert tryptophan into kynurenine (36, 37), which is involved in the immune escape mechanism (38, 39). This indicates that the tryptophan and the kynurenine pathway play an important role in tumor progression and immune response. Previous reports confirm the increased tryptophan metabolism in high-grade meningiomas (13, 14). In line with reported findings, we confirm the increased tryptophan metabolism in high-grade meningiomas (grade II and III) but also identified benign meningiomas with an upregulated choline and tryptophan metabolism. This insight provides a possible rationale suggesting that some benign classified meningioma manifest a less favorable course than others.

Taken together our presented data suggest an important role of tumor metabolism in meningiomas, only partially overlapping with respect to their histological grading. We addressed the questions as to how metabolic changes in meningiomas can provide a possible explanation for different clinical features within these histologically classified tumors. Our metabolic profiling revealed distinct subgroups marked by different activated metabolic programs. Patients with predominantly activation of the glycine-serine metabolism showed favorable grading and low proliferation index. The second metabolic subgroups were marked by choline and tryptophan metabolism, which mainly contained high-grade meningiomas but also some lower-grade tumors. The presented study is limited by the relatively low number of enrolled patients and the short follow-up time. However, although meningiomas of the WHO grade II and III are rare, we were able to include 15 patients in this study. A re-evaluation with longer follow-up should be carried out to confirm these results. In summary, our results suggest, that tumor malignancy is reflected by metabolic alterations that can support histological classifications in order to predict the clinical outcome of patients with meningiomas.

Abbreviations

NMR: Nuclear Magnetic Resonance

WHO: World Health Organization

IGF1R: Insulin-Growth-Factor1-Receptor

PFK: Phosphofructokinase

LDH: Lactate Dehydrogenase

H-NMR: Hydrogen Nuclear Magnetic Resonance

ppm: parts per million

pQ: pseudo-counted Quantile

WCNA: Weighted Correlation Network Analysis

kME: intramodule connectivity

MSEA: Metabolite Set Enrichment Analysis

HR-MAS: High Resolution Magic Angle Spinning

ROS: Reactive Oxygen Species

5-HT: 5-Hydroxytryptamine

KYN: Kynurenine

Declarations

Acknowledgement

We thank the “Struktur- and Innovationsfonds für die Forschung Baden-Württemberg” (SI-BW) and the DFG for financing NMR instrumentation that is operated within the MagRes Center of the University of Freiburg.

Ethical Approval

For this study, we included 43 patients who underwent surgery at the Department of Neurosurgery of the Medical Center, University of Freiburg. The local ethics committee of the University of Freiburg approved data evaluation, imaging procedures and experimental design (protocol 100020/09 and 5565/15). The methods were carried out in accordance with the approved guidelines. Written informed consent was obtained. The studies were approved by an institutional review board.

Consent for publication

All authors read and approved the final manuscript.

Availability of data and material for publication

Further information and requests for resources, raw data and reagents should be directed and will be fulfilled by contacting D. H. Heiland, dieter.henrik.heiland@uniklinik-freiburg.de. A full table of all materials is given in the supplementary information.

Competing interests

No potential conflicts of interest were disclosed by the authors.

Funding

DHH is funded by the German Cancer Society (Seeding Grand TII) and Müller-Fahnenberg-Stiftung.

Author's contributions

WM drafted the manuscript and participated in the data collection. KD, JW, NP conducted the laboratory tests. DD participated in the preparation of the manuscript and in the data collection. MTK participated in the design of the figures. OS and JB participated in the preparation of this article by revising it with regard to important intellectual content. DHH and JG coordinated the study and revised the article for important intellectual content.

Acknowledgement

Written consent to publish the study was obtained from the patient.

FINANCIAL SUPPORT

DHH is funded by the German Cancer Society (Seeding Grand TII) and Müller-Fahnenberg-Stiftung.

DISCLOSURE OF CONFLICTS OF INTEREST

No potential conflicts of interest were disclosed by the authors.

References

1. Modha A GP. Diagnosis and treatment of atypical and anaplastic meningiomas: a review. Neurosurgery. 2005;57:538–50.
2. Louis DN, Perry A, Reifenberger G, von Deimling A, Figarella-Branger D, Cavenee WK, et al. The 2016 World Health Organization Classification of Tumors of the Central Nervous System: a summary. Acta Neuropathol. Springer Berlin Heidelberg; 2016;131:803–20.
3. Perry A, Scheithauer B, Stafford S, Lohse C, Wollan P. "Malignancy" in meningiomas: a clinicopathologic study of 116 patients, with grading implications. Cancer. 1999;85:2046–56.
4. Clark V, Harmancı A, Bai H, Youngblood M, Lee T, Baranoski J, et al. Recurrent somatic mutations in POLR2A define a distinct subset of meningiomas. Nat Genet. 2016;48:1253–9.
5. Brastianos P, Horowitz P, Santagata S, Jones R, Mckenna A, Getz G, et al. Genomic sequencing of meningiomas identifies oncogenic SMO and AKT1 mutations. Nat Genet. 2013;45:285–289.
6. Dumanski J, Rouleau G, Nordenskjold M, Collins V. Molecular genetic analysis of chromosome 22 in 81 cases of meningioma. Cancer. 1990;res 50:5863–7.

7. Lopez-Gines C, Cerda-Nicolas M, Gil-Benso R, Callaghan R, Collado M. Association of loss of 1p and alterations of chromosome 14 in meningioma progression. Cancer Genet Cytogenet. 2004;148:123–128.
8. Perry A, Gutmann D, Reifenberger G. Molecular pathogenesis of meningiomas. J Neurooncol. 2004;70:183–202.
9. Pfisterer W, Coons S, Aboul-Enein F, Hendricks W, Scheck A. Pfisterer WK, Coons SW, Aboul-Enein F, Hendricks WP, Scheck AC, et al. (2008) Implicating chromosomal aberrations with meningioma growth and recurrence: results from FISH and MIB-I analysis of grades I and II meningioma tissue. J Neurooncol 87: 43–50. J Neurooncol. 2008;87:43–50.
10. Monleón D, Morales JM, Gonzalez-Segura A, Gonzalez-Darder JM, Gil-Benso R, Cerdá-Nicolás M, et al. Metabolic aggressiveness in benign meningiomas with chromosomal instabilities. Cancer Res. 2010;70:8426–34.
11. Serna E, Morales JM, Mata M, Gonzalez-Darder J, San Miguel T, Gil-Benso R, et al. Gene Expression Profiles of Metabolic Aggressiveness and Tumor Recurrence in Benign Meningioma. PLoS One. 2013;8.
12. Herting B, Meixensberger J, Roggendorf W, Reichmann H. Metabolic patterns in meningiomas. J Neurooncol. 2003;65:119–23.
13. Bosnyák E, Kamson DO, Guastella AR, Varadarajan K, Robinette NL, Kupsky WJ, et al. Molecular imaging correlates of tryptophan metabolism via the kynurenine pathway in human meningiomas. Neuro Oncol. 2015;17:1284–92.
14. Zitron IM, Kamson DO, Kiousis S, Juhász C, Mittal S. In vivo metabolism of tryptophan in meningiomas is mediated by indoleamine 2,3-dioxygenase 1. Cancer Biol Ther. 2013;14:333–9.
15. Beckonert O, Keun HC, Ebbels TMD, Bundy J, Holmes E, Lindon JC, et al. Metabolic profiling, metabolomic and metabonomic procedures for NMR spectroscopy of urine, plasma, serum and tissue extracts. Nat Protoc. 2007;2:2692–703.
16. Hwang TL, Shaka AJ. Water Suppression That Works. Excitation Sculpting Using Arbitrary Wave-Forms and Pulsed-Field Gradients. J. Magn. Reson. Ser. A. 1995. page 275–9.
17. Heiland DH, Wörner J, Gerrit Haaker J, Delev D, Pompe N, Mercas B, et al. The integrative metabolomic-transcriptomic glioblastome multiforme landscape of. Oncotarget. 2017;8:49178–90.
18. Hao J, Liebeke M, Astle W, De Iorio M, Bundy JG, Ebbels TMD. Bayesian deconvolution and quantification of metabolites in complex 1D NMR spectra using BATMAN. Nat Protoc. 2014;9:1416–27.
19. Hastie TJ, Narasimhan B, Tibshirani RJ, Chu G. Predictive Analysis of Microarrays. 2002;1–41.
20. McCullagh P, Nelder JA. Generalized Linear Models, Second Edition. Gen Linear Model. 1989;500.
21. Langfelder P, Horvath S. WGCNA: an R package for weighted correlation network analysis. BMC Bioinformatics. 2008;9:559.

22. Holtman IR, Raj DD, Miller JA, Schaafsma W, Yin Z, Brouwer N, et al. Induction of a common microglia gene expression signature by aging and neurodegenerative conditions: a co-expression meta-analysis. Acta Neuropathol Commun. 2015;3:31.
23. Iancu OD, Colville A, Oberbeck D, Darakjian P, McWeeney SK, Hitzemann R. Cosplicing network analysis of mammalian brain RNA-Seq data utilizing WGCNA and Mantel correlations. Front Genet. 2015;6:174.
24. Heiland DH, Mader I, Schlosser P, Pfeifer D, Carro MS, Lange T, et al. Integrative Network-based Analysis of Magnetic Resonance Spectroscopy and Genome Wide Expression in Glioblastoma multiforme. Sci Rep. 2016;6:29052.
25. Luo W, Brouwer C. Pathview: An R/Bioconductor package for pathway-based data integration and visualization. Bioinformatics. 2013;29:1830–1.
26. Monleo D, Morales M, Talamantes F, Cerda M. Benign and Atypical Meningioma Metabolic Signatures by High-Resolution Magic-Angle Spinning Molecular Profiling research articles. J Proteome Res. 2008;2882–8.
27. Antonov A, Amelio I, Cutruzzola F, Agostini M, Melino G. Serine and glycine metabolism in cancer. 2014;39:191–8.
28. Gut P, Verdin E. The nexus of chromatin regulation and intermediary metabolism. Nature. 2013;502:489–96.
29. Cheng L, Chang I, Louis D, Gonzalez R. Correlation of high-resolution magic angle spinning proton magnetic resonance spectroscopy with histopathology of intact human brain tumor specimens. Cancer Res. 1998;58:1825–1832.
30. PFISTERER W, NIEMAN R, SCHECK A, COONS S, SPETZLER R, PREUL Mcd. Using ex vivo proton magnetic resonance spectroscopy to reveal associations between biochemical and biological features of meningiomas. 2010;28:1–8.
31. Pfisterer WK, Hendricks WP. Fluorescent in situ hybridization and ex vivo H Magnetic Resonance Spectroscopic examination of meningioma tumor tissue: is it possible to identify a clinically-aggressive subset of benign meningiomas? 2018;61:1048–61.
32. Gillies R, Barry J, Ross B. In vitro and in vivo 13C and 31P NMR analyses of phosphocholine metabolism in rat glioma cells. Magn Reson Med. 1994;310–318.
33. Preul M, Caramanos Z, Collins D, Villemure J, Leblanc R, Olivier A, et al. Accurate, noninvasive diagnosis of human brain tumors by using proton magnetic resonance spectroscopy. Nat Med. 1996;323–5.
34. Mishra G, Phatak S, Kakde D. ROLE OF MAGNETIC RESONANCE SPECTROSCOPY IN CLASSIFYING MENINGIOMAS WITH HISTOPATHOLOGICAL CORRELATION. Int J Sci Res. 2018;203–5.
35. Mefford I, Barchas J. Determination of tryptophan and metabolites in rat brain and pineal tissue by reversed-phase highperformance liquid chromatography with electrochemical detection. J Chromatogr. 1980;187–193.

36. Metz R, Duhadaway J, Kamasani U, Laury-Kleintop L, Muller A, Prendergast G. Novel tryptophan catabolic enzyme IDO2 is the preferred biochemical target of the antitumor indole amine 2,3-dioxygenase inhibitory compound d-1-methyl-tryptophan. Cancer Res. 2007;7082–7087.
37. de Jong R, Nijman H, Boezen H, Volmer M, Ten Hoor K, Krijnen J, et al. Serum tryptophan and kynurenine concentrations as parameters for indoleamine 2,3-dioxygenase activity in patients with endometrial, ovarian, and vuluar cancer. Int J Gynecol Cancer. 2011;1320– 1327.
38. Sucher R, Kurz K, Weiss G, Margreiter R, Fuchs D, Brandacher G. IDO-mediated tryptophan degradation in the pathogenesis of malignant tumor disease. Int J Tryptophan Res. 2010;113–120.
39. Prendergast G. Cancer: why tumours eat tryptophan. Nature 478:192–194. Nature. 2011;192–194.

Table

Table 1

Parameter		Claster 1 N = 15	Claster 2 N = 28	Significance level (p)
Sex (N,%)				
	Male (N = 10)	2 (14.2%)	8 (28.5%)	0.45****
	Femal (N = 33)	13 (86.6%)	20 (71.4%)	
Age (mean, SD)		62.3 ± 13.1	64.4 ± 12.8	0.62*
Size (cm^3) (mean, SD)		48.3 ± 51.8	88.6 ± 103.3	0.09*
Peritumoral edema (N, %)				
	high	4(26.6%)	18(64.3%)	**0.02*** **
	low	11(73.4%)	10(35.7%)	
Location (N, %)				
	falx	3(20%)	3(10.7%)	0.64****
	convexity	2(13.3%)	10(35.7%)	0.16****
	frontobasal	4(26.6%)	5(17.8%)	0.69****
	sphenoid wing	2(13.3%)	4(14.2%)	1***
	petroclival	1(6.6%)	1(3.5%)	1****
	spinal	2(13.3%)	1(3.5%)	0.11****
	others	1(6.6%)	4(14.2%)	0.64****

SD: standard deviation

CI: confidence interval

KPS: Karnofsky score

* T-test

**Wilcoxon test

***Chi-squared test

****Fisher's exact test

Parameter		Claster 1 N = 15	Claster 2 N = 28	Significance level (p)
Simpson grad (N, %)				
	Grade 1	5(33.3%)	7(25%)	0.74****
	Grade 2	9(60%)	16(57.1%)	1***
	Grade 3	0(0%)	3(10.7%)	0.54****
	Grade 4	1(6.6%)	2(7.1%)	1****
Preoperative KPS (median, 95% CI)		80% CI(70%-80%)	70% CI(%60–80%)	**0.01****
Postoperative KPS (median, 95% CI)		90% CI(80%-90%)	70% CI(50%-90%)	**0.007****
Proliferation index (N, %)				
	MIB1 < 5%	15(100%)	9(32.1%)	**0.01****
	MIB1 > 5%	0(0%)	19(67.9%)	
Pathology (N, %)				
	WHO grade I	15(100%)	13(46.4%)	**0.001****
	WHO grade II + III	0(0%)	15(53.6%)	
SD: standard deviation				
CI: confidence interval				
KPS: Karnofsky score				
* T-test				
**Wilcoxon test				
***Chi-squared test				
****Fisher’s exact test				

Figures

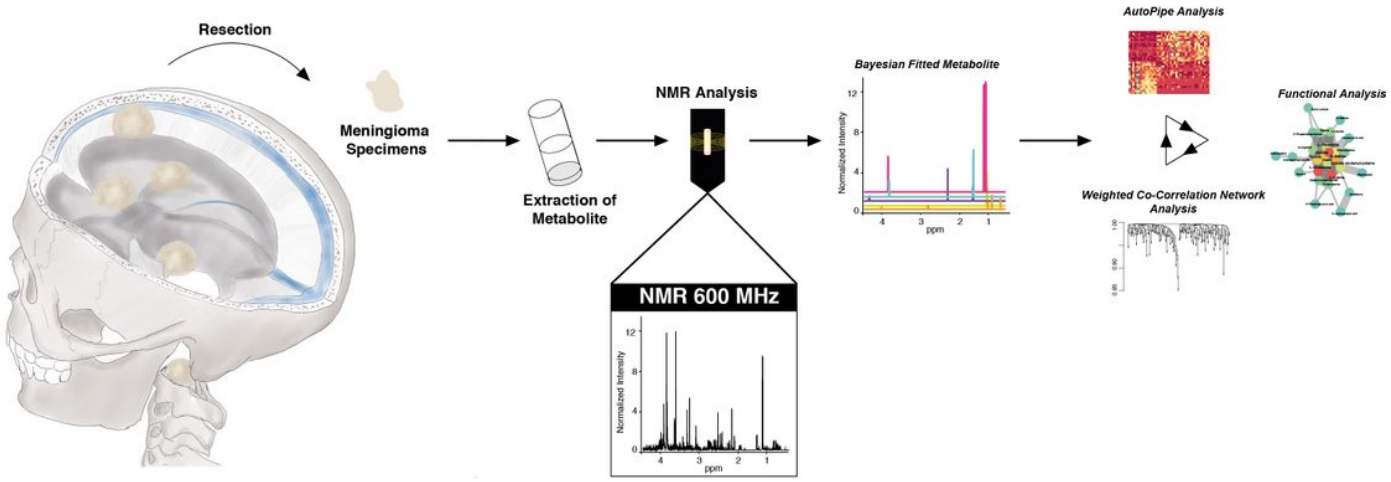

Figure 1

Workflow of metabolite extraction, identification of metabolite and bioinformatical analysis. The extracted specimens are analyzed by NMR analysis. Metabolite are fitted and further analyzed by unsupervised clustering and network analysis.

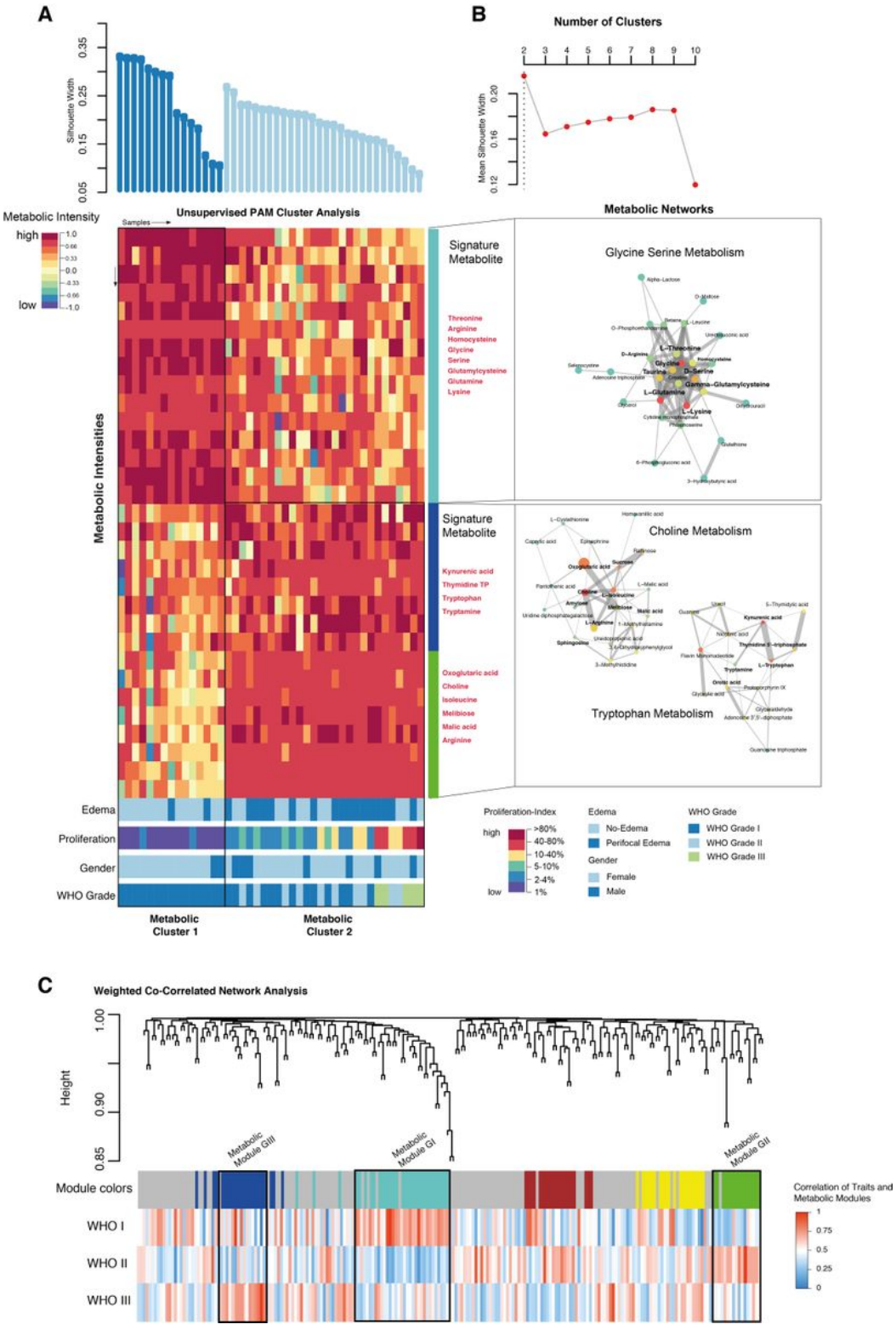

Figure 2

A. In the upper plot, the silhouette widths of both clusters are shown ordered by different cluster subgroups. In the middle panel, a heatmap illustrate the metabolic intensity of the top ranked metabolites. At the bottom panel, the information on clinical properties is available. These are color-coded and explained in the side panel. B. In the upper panel, the plot illustrates the optimal number of clusters. The optimal number of clusters was achieved by PAM clustering from 2 to 10 number of clusters

by calculating the mean silhouette widths. In the bottom panel, a network analysis of the metabolic pathways highly enriched in cluster 1 and 2 respectively is given. C. A weighted correlation network analysis (WGNC) was performed to explore the associated clinical features and molecular/metabolic, further detailed interpretation of all identified modules is given in the supplementary data.

Supplementary Files

This is a list of supplementary files associated with this preprint. Click to download.

- Supplementary.docx